

SIMULTANEOUS OPTIMIZATION OF AIRFRAME AND ENGINE FOR SUPERSONIC TRANSPORT

Atsushi UENO*, Yasushi WATANABE*

*Japan Aerospace Exploration Agency

aueno@chofu.jaxa.jp;wata@chofu.jaxa.jp

Keywords: SST, Optimization, Aerodynamic performance, Engine performance

Abstract

JAXA is developing a multidisciplinary design optimization (MDO) tool for airframe-propulsion integration of future supersonic transports. This MDO tool has characteristics of considering economic efficiency and environmental compatibility that are considered to be reasons the Concorde failed to produce commercial success. In this MDO tool, specifications of airframe and engine (e.g., wing span and bypass ratio) are simultaneously optimized to satisfy mission and environmental requirements.

This paper describes the method used in this tool and results of optimization study. In the optimization study, the cruising range is the index to economic efficiency and the index of environmental compatibility is airport noise. Results show that the turbine inlet temperature has large effect on vehicle weight. Results also show that this tool has room for improvement. The points of improvement are summarized at the end of this paper.

1 Introduction

JAXA is performing a flight demonstration program as well as a basic research program to realize economically-viable, environmentally-friendly small supersonic transport [1]. The specification of the first configuration of JAXA’s small supersonic transport (QSST) is shown in Table 1.


One of the reasons the Concorde failed to produce commercial success is that the flight route was restricted due to lack of cruising range and large airport noise. So the investigation considering both cruising range

and airport noise is needed from the viewpoints of economic efficiency and environmental compatibility. The cruising range depends on both airframe performance (e.g., lift-to-drag ratio (L/D)) and engine performance (e.g., specific fuel consumption (SFC)), which shows the importance of airframe / propulsion integration.

JAXA is developing a multidisciplinary design optimization (MDO) tool for supersonic transports. In this tool, specifications of airframe and engine are optimized based on a mission analysis that simultaneously considers airframe and engine performance. The objective function in the optimization study is the cruising range, and the airport noise is the constraint function. Currently, this MDO tool includes three modules such as “aerodynamic analysis”, “engine cycle analysis”, and “weight analysis”, to evaluate the cruising range, and the airport noise is represented by the engine noise that is evaluated by the exhaust velocity.

In this paper, the outline of this MDO tool is described and results of optimization study are discussed. Finally, the future work revealed through the optimization study is summarized.

Table 1. Specification of JAXA QSST

Length	48 m	
Span	23 m	
Weight	70 ton	
Speed	1.6 Mach	
Range	3500 nm	
Passenger	30-50	

2 Outline of MDO Tool

The flow diagram of this MDO tool is shown in Fig. 1. Specifications of airframe and engine are

set within the design space shown in Table 2. Then, the aerodynamic performance, engine performance, and weight are evaluated and the mission analysis is performed to obtain the cruising range and take-off performance. The Pareto-optimal solutions with respect to the cruising range and weight are explored by using the genetic algorithm, while airport noise and take-off performance are constrained to satisfy the regulations.

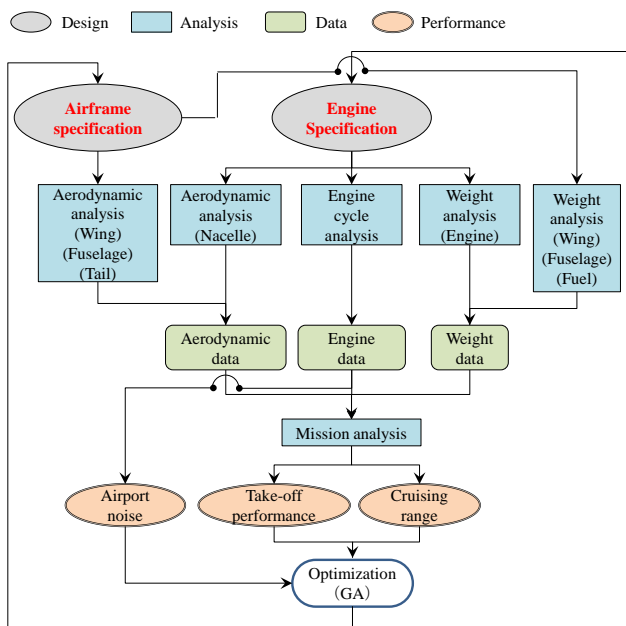


Fig. 1. Flow diagram of MDO tool

L/D is important in designing airframe shape and is also important in setting engine specifications because required thrust depends on L/D. L/D strongly depends on the wing planform. Therefore, the wing planform was chosen as the design variables of airframe. Specifically, design variables are $B2$: span, $B1$: inner wing span divided by span, Cr : chord length at root, Ck : chord length at kink, $A1$: sweepback angle of inner wing, $A2$: sweepback angle of outer wing, and Xt : wing position (Fig. 2 and Table 2). In Table 2, specifications of first configuration of QSST are shown in parenthesis. Specifications other than shown above were fixed in the optimization study and were defined as follows. The airfoil is NACA 6 series having thickness to chord ratio of 3%. The dihedral angles of inner and outer wings are 9 and 3 degrees, respectively. The fuselage is similar to that of the flight test model in D-SEND#2

project conducted by JAXA. The high lift device is installed at the trailing edge of the wing. The horizontal tail is the flying tail (Fig. 2). The vertical tail is not modeled in this MDO tool because only the longitudinal motion is considered. In this paper, the shape having the wing of first configuration of QSST and also having fuselage and horizontal tail shown above is referred to as the reference shape.

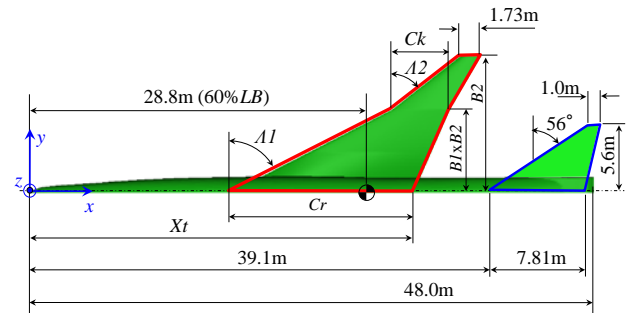


Fig. 2. Design variables of airframe

Table 2. Range of design variables*

Wing Planform		Engine	
$B1$	0.2 ~ 0.9 (0.61)	BPR	1.0 ~ 4.0
$B2$, m	10 ~ 14 (11.56)	TIT , deg C	1500~1700
Cr , m	12 ~ 18 (15.60)	AF , m ²	1.0 ~ 3.0
Ck , m	3 ~ 7 (4.89)	$RSLR$	2.5 ~ 4.5
Xt , m	31 ~ 37 (32.65)	$RTRN$	0.6 ~ 1.1
$A1$, deg	50 ~ 70 (63.0)		
$A2$, deg	30 ~ 55 (52.0)		

* Specifications of first configuration of QSST are shown in parenthesis.

The engine is the mixed-flow, two-shaft turbofan engine having fixed cycle without reheat. The design variables are BPR : bypass ratio, TIT : turbine inlet temperature, AF : fan area, and $RSLR$, $RTRN$: thrust ratios (Table 2). The engine performance is evaluated at following three conditions; 1) at sea level / static (SLS), 2) at an altitude of 36kft / Mach 0.9, and 3) at an altitude of 50kft / Mach 1.6. $RSLR$ is thrust at condition 1) divided by thrust at condition 3). Similarly, $RTRN$ is thrust at condition 2) divided by thrust at condition 3). Here, the fan pressure ratio (FPR) and compressor pressure ratio (CPR) are important specification determining thermodynamic cycle. However, FPR and CPR strongly depend on the number of stages. Based on the engines studied for supersonic transports, the number of stages

of fan and compressor were set to 2 and 9, respectively and *FPR* and *CPR* were fixed at 2 and 15, respectively.

3 Method of Analysis

In this chapter, methods of aerodynamic analysis, engine cycles analysis, weight analysis, and mission analysis are shown. Results of validation analysis are also shown.

3.1 Aerodynamic Analysis

The outline of aerodynamic analysis is shown in Fig. 3. The aerodynamic coefficients are divided into those of basic characteristics, horizontal tail effectiveness, and flap effectiveness. The reference area is the wing area (surrounded by red line in Fig. 2). The longitudinal reference length is the body length. The moment reference center is located at $x=28.8\text{m}$ (Fig. 2).

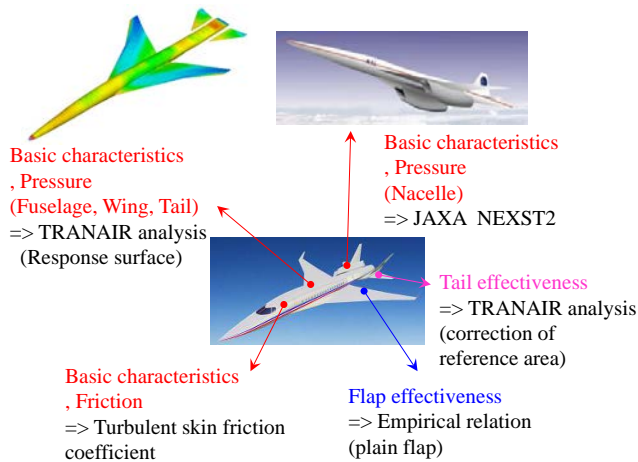


Fig. 3. Outline of aerodynamic analysis

[Basic characteristics]

The aerodynamic coefficients due to pressure consist of those of clean configuration (body, wing, and horizontal tail) and those of nacelle. Here, interference effect between clean configuration and nacelle is not considered. The aerodynamic coefficients of clean configuration are evaluated by commercial software ‘Tranair’. Tranair needs less computation time than Euler analysis. However, it is unpractical to execute Tranair in the optimization loop. Thus, the response surface based on the result of Tranair is constructed and used in the optimization

study. The nacelle is assumed to produce only drag and its drag coefficient is estimated by using the drag coefficient of nacelle calculated in JAXA’s NEXST 2 project.

The drag coefficient due to friction ($C_{D,f}$) is evaluated by using the empirical relation based on the turbulent skin friction coefficient on a flat plate [2] (Eq. (1)).

$$C_{D,f} = 0.455 \log_{10}(Re)^{-2.58} (1 + 0.144M^2)^{-0.65} \left(\frac{S_{wet}}{S_{ref}} \right) \quad (1)$$

[Horizontal tail effectiveness]

The horizontal tail effectiveness of the reference shape is evaluated at horizontal tail angle of ± 5 degrees by Tranair. The horizontal tail effectiveness depends on the wing planform. However, the horizontal tail effectiveness of the reference shape is used with correction of reference area even when the wing planform is changed from the reference shape.

[Flap effectiveness]

The flap effectiveness is used in the evaluation of take-off performance (balanced field length and climb gradient at the second take-off segment) shown in section 3.4. The maximum lift coefficient and L/D are required in order to evaluate take-off performance. The increment of maximum lift coefficient by flap deflection ($\Delta C_{L,max}$) is estimated by Eq. (2) [2].

$$\Delta C_{L,max} = 0.9 \Delta C_{l,max} \left(\frac{S_{flapped}}{S_{ref}} \right) \cos \Lambda_{H.L.} \quad (2)$$

, where $\Delta C_{l,max}$ in Eq. (2) is fixed at 0.9. The ratio of effective area of flap to reference area ($S_{flapped}/S_{ref}$) is fixed at 1/3. The angle of hinge line of flap ($\Lambda_{H.L.}$) is calculated on the condition that the hinge line is parallel to the trailing edge of wing.

Regarding L/D, it is reported that L/D of double-delta wing is increased by about 20% by flap deflection of trailing edge flap [3] (Here, L/D is evaluated at $C_L=0.6$ that is supposed to be used at take-off.). Thus, L/D with flap deflection at the second take-off segment is increased by 20% from that of basic characteristics.

3.2 Engine Cycle Analysis

The engine performance such as thrust and SFC is calculated by the thermodynamic cycle analysis [4]. In the thermodynamic cycle analysis, the segments from air inlet to nozzle are considered (Fig. 4), but the mechanical constraints such as number of revolutions are not considered.

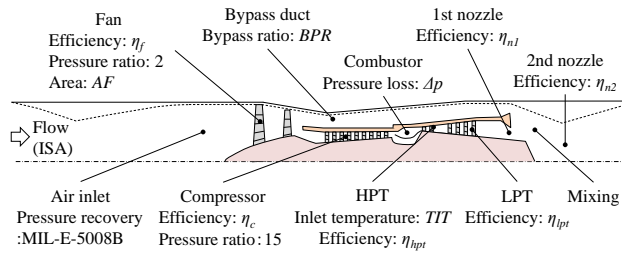


Fig. 4. Outline of engine cycle analysis

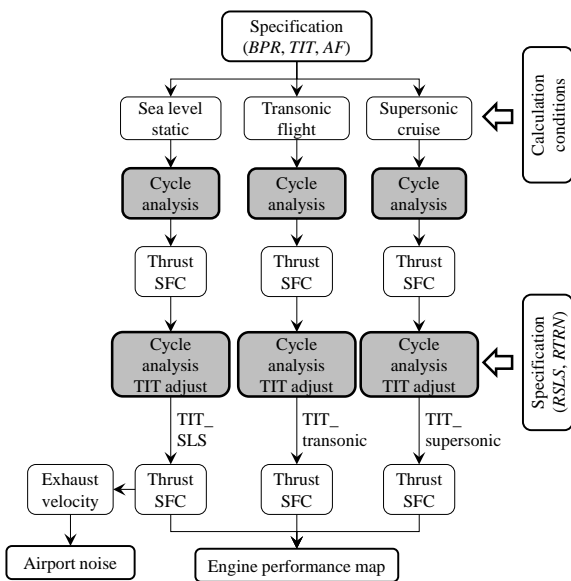


Fig. 5. Flow diagram of evaluation of engine performance

Initially, the thrust and SFC are obtained at three conditions shown in section 2 by the thermodynamic cycle analysis based on engine specification that is given as design variable (Fig. 5). Then, the turbine inlet temperatures at three conditions are adjusted to realize the thrust ratio ($RSLS$, $RTRN$). In this adjustment, the turbine inlet temperature (TIT) at any one of three conditions corresponds to TIT that is given as design variable, and TIT at remaining conditions are lower than that. This adjustment reveals the critical operation condition at which

the TIT is the maximum. Finally, the engine performance map (thrust and SFC as a function of altitude and Mach number) is made based on the engine performance at three conditions by using engine performance map made for SSBJ in the previous study.

The airport noise is represented by the engine noise that is evaluated by the exhaust velocity at SLS condition. In the optimization study, the exhaust velocity rather than airport noise is constrained.

3.3 Weight Analysis

The weight analysis is based on the result for first configuration of QSST (Table 3).

Table 3. Weight data

Component	Weight, ton	Component	Weight, ton
Fuselage	3.1	Engine	10.0
Wing	8.5	Fuel	33.8
Tail	0.9	Payload	5.0
Nacelle	1.4	Other	7.3

In this tool, design variables are specifications of wing planform and engine. Thus, weight of fuselage, tail, nacelle, payload, and other is fixed at values shown in Table 3, and weight of wing, engine, and fuel is estimated as follows.

The weight of wing is based on Eq. (3) [2].

$$W_{wing} \propto S_w^{0.622} A^{0.785} (1 + \lambda)^{0.05} (\cos \Lambda)^{-1} \quad (3)$$

, where S_w is wing area, A is aspect ratio, λ is taper ratio, and Λ is sweepback angle. First, the ratio of right-hand value to that of first configuration of QSST is calculated. Then, the resultant ratio multiplied by 8.5 ton (weight of wing of first configuration of QSST) gives weight of wing. Fuel is stored in the wing, and fuel weight is assumed to be proportional to the 1.5th power of wing area. Engine weight is based on the thrust to weight ratio of engine that is a function of turbine inlet temperature and bypass ratio. The position of center of gravity including its travel during the flight is not modeled. Currently, the position of center of gravity is fixed at $x=28.8m$ (60% LB) (Fig. 2).

3.4 Mission Analysis

In the mission analysis, the balanced field length (BFL), the climb gradient at second take-off segment, and the cruising range are calculated.

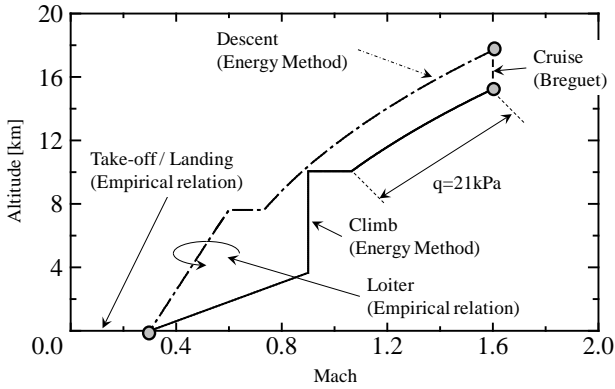


Fig. 6. Outline of mission analysis

[Balanced field length]

BFL is calculated by the point mass analysis. The lift and drag coefficients during ground run are assumed to be zero and 0.03, respectively. The ground friction coefficients at acceleration and deceleration phases are assumed to be 0.05 and 0.3, respectively. The angle of attack after lift-off is fixed at 12 degrees, and the lift coefficient is increased from that of basic characteristics by $\Delta C_{L,max}$ due to the flap deflection. L/D is also increased by 20% from that of basic characteristics due to the flap deflection.

[Climb gradient at second take-off segment]

The climb gradient at second take-off segment is calculated by the point mass analysis considering force balance in the directions of velocity and flight-path angle. The thrust is reduced by 13% from the SLS thrust, because the thrust is normally decreased as the flight velocity is increased. L/D is increased by 20% as is described in the calculation of BFL.

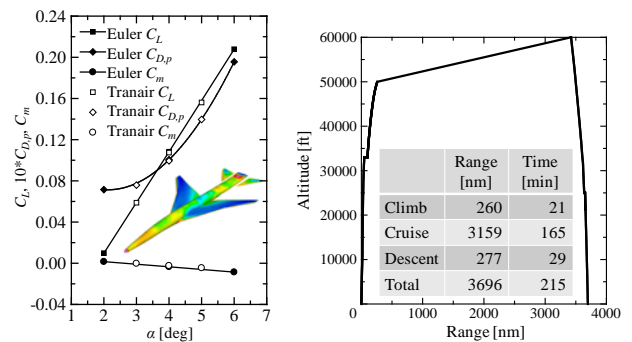
[Cruising range]

The calculation of cruising range is divided into 6 phases shown in Fig. 6. The reserve fuel is assumed to be 10% of total fuel. The flight

path can be defined arbitrarily. In this paper, the flight path shown in Fig. 6 is used. The fuel consumptions in take-off, loiter, and landing phases are calculated by the empirical relation [2]. In climb and descent phases, the fuel consumption and cruising range are calculated by the energy method [5]. The Breguet's range equation gives the range in the cruise phase.

3.5 Validation

The aerodynamic coefficients of the reference shape obtained by Tranair agree well with the results of Euler analysis (Fig. 7). The differences of thrust and SFC between this MDO tool and high fidelity tool developed by engine manufacturer are within 10%. The validation analysis is not performed for the weight analysis, because the empirical relations are used. The validation analysis of the mission analysis is based on the data of the Concorde. At the cruise, L/D is 7.1, and SFC is 1.195. The take-off weight and fuel weight are 185 ton and 95.7 ton, respectively. The resultant cruising range is 3690 nm that is 5% smaller than the actual range (3900nm).



(a) Aerodynamics (b) Mission analysis

Fig. 7. Validation of MDO tool

4 Optimization study

The optimization study is performed by using this MDO tool, and the optimal specifications of airframe and engine are explored from the viewpoints of economic efficiency (cruising range) and environmental compatibility (airport noise).

4.1 Definition of Optimization Problem

The optimization problem is shown in Table 4.

Table 4. Optimization problem

Objective Function		Design Variable	
Weight	Minimize	Airframe	
Constraint Function		<i>B1</i>	0.2 ~ 0.9
Range	= 3500 nm	<i>B2</i> , m	10 ~ 14
<i>Vj</i>	(*)	<i>Cr</i> , m	12 ~ 18
BFL	<7000 ft	<i>Ck</i> , m	3 ~ 7
Gradient	>3.6 %	<i>Xt</i> , m	31 ~ 37
Time	<25 min	<i>A1</i> , deg	50 ~ 70
Stability	positive	<i>A2</i> , deg	30 ~ 55
		Engine	
		<i>BPR</i>	1.0 ~ 4.0
		<i>TIT</i> , deg C	1500~1700
		<i>AF</i> , m ²	1.0 ~ 3.0
		<i>RSLs</i>	2.5 ~ 4.5
		<i>RTRN</i>	0.6 ~ 1.1

(*) Multiple values of *Vj* are defined.

The weight is minimized under six constraint functions. The design variables are the same as shown in Table 2. Regarding constraint functions, the constraint value of cruising range is 3500nm that is the target cruising range of JAXA’s QSST. Multiple constraint values of exhaust velocity (*Vj*) are defined in order to investigate effect of *Vj* on specifications of airframe and engine. Here, *Vj_C3* and *Vj_C4* are defined as the exhaust velocities that satisfy the noise regulation of ICAO’s Chapter 3 and 4, respectively. The constraint value of climb gradient at second take-off segment is 3.6% that is 50% larger than FAR’s required climb gradient (2.4% for twin jet). The calculation of the climb gradient shown in section 3.4 is simplified one (e.g., without the effect of tail wind). Thus, large margin is applied. Time shown in Table 4 is the flight time in the climb phase. The preliminary analysis shows that the maximum turbine inlet temperature within the design space is the best. Thus, the turbine inlet temperature (*TIT*) is fixed at 1500 and 1700 deg C to investigate the effect of *TIT* on other specifications.

4.2 Result and Discussion

The optimization study was performed with three different constraint values for *Vj*

($V_{j1}=V_{j_C4} < V_{j2} < V_{j_C3} < V_{j3}$). The results are shown in Table 5 and Figs. 8 and 9.

Table 5. Specification of optimum solution

Jet Velocity	<i>Vj1</i>	<i>Vj2</i>	<i>Vj3</i>	<i>Vj1</i>
Weight, ton	72.28	72.10	72.00	76.66
Wing Area, m ²	191.2	192.1	192.6	200.5
BFL, ft	6207	6153	6251	6302
Gradient, %	3.6	3.8	3.8	3.6
Time, min	24.8	24.9	24.9	24.7
Stability	positive	positive	positive	positive
<i>BPR</i>	3.05	2.86	2.69	2.18
<i>TIT</i> , deg C	1700	1700	1700	1500
<i>AF</i> , m ²	2.63	2.50	2.38	2.81
<i>RSLs</i>	3.50	3.55	3.62	3.47
<i>RTRN</i>	0.88	0.90	0.97	0.83

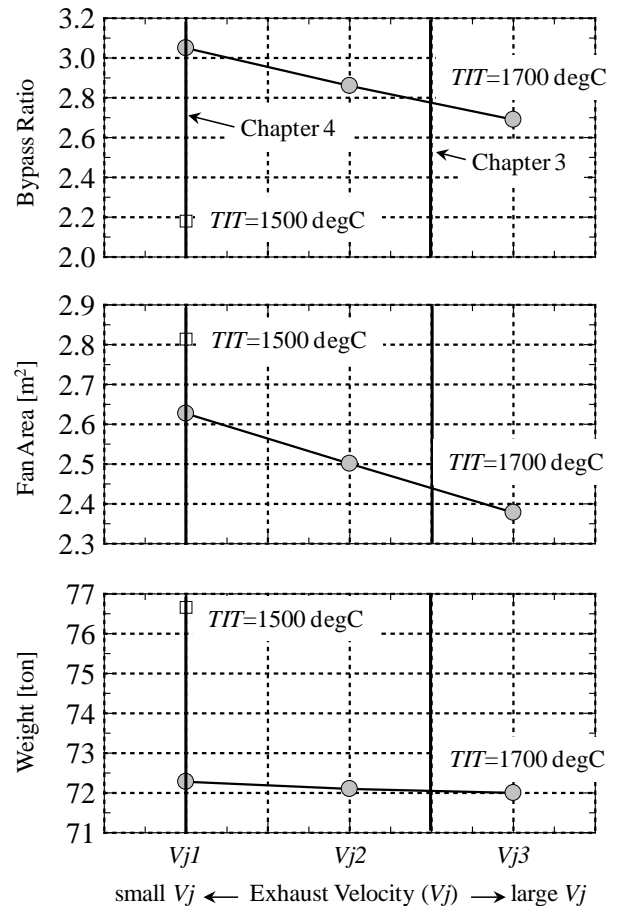


Fig. 8. Specification of optimum solution

[Effect of *Vj*]

The effect of airport noise (*Vj*) on the specification setting is discussed based on the result obtained at *TIT*=1700 deg C. Regarding engine specifications, as the constraint of airport noise becomes severe, the bypass ratio (*BPR*) and fan area (*AF*) become large, while the thrust

ratio (*RSLs*, *RTRN*) becomes small (Table 5). *BPR* tends to become large to reduce the exhaust velocity, and this trend appears in this study. The mass flow provided to engine is determined by *AF*, and the mass flow should be increased to produce required thrust when the exhaust velocity is reduced. Consequently, *AF* becomes large as the exhaust velocity is reduced. The reason for the decrease of *RSLs* (SLS thrust divided by cruise thrust) and *RTRN* (transonic thrust divided by cruise thrust) is mainly the difference of required thrust, as described below. The difference of weight between cases of *Vj1* and *Vj3* is small (+0.4%, Table 5), and therefore, the difference of SLS thrust is also small. As the exhaust velocity becomes small, *BPR* becomes large, which reduces fuel consumption. As a result, the difference of weight at the beginning of cruise (+1.0%) is relatively large compared to that at SLS (+0.4%). Consequently, small exhaust velocity requires large cruise thrust, which leads to the decrease of thrust ratio (*RSLs*, *RTRN*). Here, the cruise thrust depends on weight as well as L/D. However, L/D is almost the same between these cases as described below, and the difference of cruise thrust is mainly caused by the difference of weight.

Regarding weight, the small exhaust velocity increases engine weight due to large *BPR* and large *AF*. On the other hand, large *BPR* reduces fuel weight, which in turn reduces wing weight. These are compensated with each other. Thus, the effect of the exhaust velocity on weight is small (Table 5).

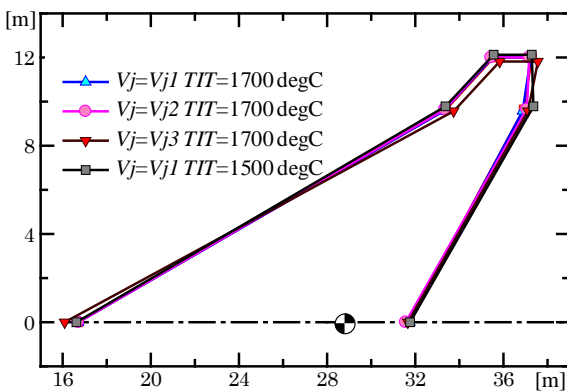


Fig. 9. Optimum wing planform

The optimal wing planform is almost the same regardless of *Vj* (Fig. 9). The constraint

function of aerodynamics (i.e., static stability) is dominant in this study, and the wing planform that realizes small trim drag and large cruise L/D with static stability is thought to be selected as the optimal one regardless of engine specifications.

[Effect of turbine inlet temperature]

The effect of *TIT* on *BPR* and weight is larger than that of *Vj* (Fig. 8). For example, weight is increased by 6.1% when *TIT* is decreased by 12% from 1700 deg C to 1500 deg C, while weight is increased by only 0.4% when *Vj* is decreased by 10% from *Vj3* to *Vj1*.

When *TIT* is small, the energy of fluid behind high and low pressure turbines is small, and the exhaust velocity of core flow becomes small. However, the exhaust velocity is constrained by *Vj*. Therefore, the bypass flow needs to be decreased and the core flow needs to be increased to satisfy the constraint of *Vj*. As a result, *BPR* becomes small as *TIT* becomes small. The small *BPR* enlarges the size of core engine, which leads to the increase in engine weight. Furthermore, the small *BPR* increases the fuel weight and the wing weight. As described above, the small *TIT* reduces *BPR*, and reduced *BPR* increases weight.

Above discussion leads to the conclusion that the large *TIT* is desirable to decrease weight, however, *TIT* should be determined considering the cooling capability of turbine and realization of heat-resistant material. *BPR* is affected by *TIT* and constraint value of *Vj*. Therefore, *BPR* should be optimized to satisfy the requirement of noise level along with usable *TIT*. In this study, the wing planform is not affected by specifications of engine and constraint value of *Vj*. Therefore, the wing planform should be designed to meet the aerodynamic requirement such as static stability and large cruise L/D.

4.3 Future Work

To realize high fidelity airframe / propulsion integration, this MDO tool should be updated according to the following requirements. 1) the analysis model (shown in rectangle box in Fig. 1) should be added to simulate the actual

environment more precisely. 2) the accuracy of each analysis model should be improved. Through the optimization study shown in section 4.2, following three points are revealed to be important.

Accuracy of aerodynamic model:

Currently, the drag of nacelle is separately calculated without consideration of interference drag between nacelle and wing. The large *BPR* reduces fuel consumption but enlarges nacelle, which increases interference drag. In the present model, only the positive effect of *BPR* (i.e., improvement in SFC) is modeled, and thus the larger *BPR* is thought to be selected as optimal one. Consequently, the aerodynamic model should be improved to include the interference drag between nacelle and wing.

Travel of center of gravity:

In this study, the constraint of aerodynamics (static stability) is dominant in designing the wing planform, and specifications of engine hardly affect the wing planform. One of the reasons for above result is that the position of center of gravity was fixed. The degree of freedom in designing the wing planform can be increased when the travel of center of gravity due to fuel transfer during flight is modeled.

Airport noise model:

The constraint of airport noise strongly affects engine specifications such as bypass ratio and fan area. However, the exhaust velocity rather than airport noise is constrained in this tool. Currently, analysis model to evaluate airport noise based on the exhaust velocity is not constructed. Airport noise model should be included in the future.

5 Conclusion

The MDO tool based on the mission analysis considering airframe / propulsion integration of supersonic transports is developed. The optimization study of specifications of airframe and engine is performed from the viewpoints of both economic efficiency (cruising range) and environmental compatibility (airport noise).

Results show that the turbine inlet temperature has large effect on vehicle weight. Results also show that the optimum bypass ratio depends on the turbine inlet temperature and airport noise. This MDO tool is planned to be improved according to the points of improvement revealed through the optimization study.

References

- [1] Murakami A. Research Activities on Supersonic Technology at JAXA. *2010 Asia-Pacific International Symposium on Aerospace Technology*. Xi'An, 2010.
- [2] Raymer D. *Aircraft Design: A Conceptual Approach*. 4th edition, AIAA Education Series, AIAA, 2006.
- [3] Kwak D, et al. Experimental Investigation of High Lift Device for SST. NAL TR-1450, 2002. (in Japanese)
- [4] Kumazawa T and Honda M. Research on Integration Performance of Supersonic Engine. Graduation thesis, Tokyo University of Science, 1991. (in Japanese)
- [5] Asselin M. *An Introduction to Aircraft Performance*. AIAA Education Series, AIAA, 1997.

Copyright Statement

The authors confirm that they, and/or their company or organization, hold copyright on all of the original material included in this paper. The authors also confirm that they have obtained permission, from the copyright holder of any third party material included in this paper, to publish it as part of their paper. The authors confirm that they give permission, or have obtained permission from the copyright holder of this paper, for the publication and distribution of this paper as part of the ICAS2012 proceedings or as individual off-prints from the proceedings.